MULTI-USER LEO-SATELLITE RECEIVER FOR ROBUST SPACE DETECTION OF AIS MESSAGES

Mu Zhou, Alle-Jan van der Veen and René van Leuken

Delft University of Technology, Dept. of Elec. Eng., Mekelweg 4, 2628 CD Delft, The Netherlands.
Email: m.zhou@tudelft.nl; a.j.vanderveen@tudelft.nl; t.g.r.m.vanleuken@tudelft.nl.

The coverage of the terrestrial automatic identification system (AIS) is limited to close areas off the coast. Low earth orbit (LEO) satellites can expand the service of AIS to a global range but it brings large variance in Doppler shift, path loss and propagation delay. The communication between ships and LEO satellites becomes asynchronous. The collision of AIS messages from thousands of ground cells results in loss of all collided messages. Previous papers discussed the use of a single user receiver to detect AIS messages under heavy co-channel interference but the problem was never well solved. In this paper, we present a multi-user receiver equipped with an antenna array on LEO satellites, which explores the spatial multiplexing in space detection of AIS messages and significantly improves the detection performance. The proposed receiver performs rank tracking and subspace intersection based on the signed URV decomposition ahead of blind source separation to provide robust separation of user data for single user receivers. The proposed receiver is tested in an exact dynamic AIS model.

Index Terms— Multi-user receiver, LEO satellite, automatic identification system, signed URV decomposition, subspace intersection.

1 INTRODUCTION

Recently, a need for global commercial goods tracking evolves the setup of an effective global tracking system. The automatic identification system (AIS) [1] is one of the candidates. AIS messages even have potential value for the defense and security purposes where one wants to collect information on ships approaching the one's coast. AIS is a narrowband communication system where ships at sea send navigational data to the base stations continuously. This system uses the self organized time division multiple access (SOTDMA) technique inside ground cells to handle the transmission in the VHF maritime mobile band. The coverage of terrestrial AIS is limited to close area about 20 to 30 nautical miles off the coast by the short detection distance away from base stations. Recent analyses [2, 3, 4, 5] show that low earth orbit (LEO) satellites can expand the service of AIS to a global range including the traffic at open sea. LEO satellites see thousands of ground cells and pass over them at a very high speed, such that they face additional technical challenges, which are the collision of messages caused by the large difference in propagation time from cells to satellites, the high Doppler shift caused by the large relative speed between ships and satellites, and the large variance in path loss due to the big satellite field of view (FoV). The communication becomes asynchronous between ships and satellites.

Many papers [6, 7, 8] discussed the use of a single user receiver on the LEO satellite equipped with one receiver antenna. This kind of receiver provides service only reliable in sparsely trafficked areas.

The paper [2] discussed the use of an antenna array to do interference cancelation by suppressing the signals from some heavy trafficked areas to improve the detection probability for other areas in FoV, but it is essentially a single user receiver and the spatial null is found by sweeping the beam, which is not in real-time.

Since the messages from ships come from random directions and at sparse time points, an antenna array on the satellite can explore the spatial multiplexing in the space detection of AIS messages by separating messages coming from different directions. Blind source separation (BSS) algorithms, which are robust to antenna calibration errors and independent of array configuration, can be used on satellites to do this separation. Unfortunately, the available BSS algorithms are originally developed for synchronous communication so they can not be directly and stably applied to this scenario.

In this paper, we present a multi-user LEO satellite receiver equipped with an antenna array to solve the above problems. This receiver performs rank tracking to determine the start of data frames, then preprocesses the received nonstationary data, and separate user data before applying the single user receiver. The rank tracking uses the subspace tracking algorithm based on the signed URV decomposition (SURV) [9]. The preprocessing uses modified subspace intersection based on SURV [10]. The separation uses algebraic constant modulus algorithm (ACMA) [11] since AIS signals have a constant envelope. The performance of the proposed receiver is tested with the exact AIS model based on the work in [12].

2 DATA MODEL

AIS message: An AIS message is typically $N_p = 256$ bits long (see Fig. 1). It has a leading training sequence (TS) consisting of alternative 0s and 1s. The start flag (SF) and end flag (EF) for information data are 8 bits long. The information data is appended with a frame check sequence (FCS), a 16-bit cyclic redundancy code (CRC). The information data and FCS are bit stuffed (a zero is inserted after every five continuous 1s). The binary sequence $\{b_n\}_{1 \leq n \leq N_p}$ of the AIS message is mapped into $\{+1, -1\}$ and then differentially encoded (NRZI encoding) as $a_n = b_n a_{n-1}, n \geq 1, a_0 = +1$. The encoded message is Gaussian minimum shift keying (GMSK) [13] modulated and transmitted at 9.6kbps on carriers at frequency 162MHz. The baseband representation of transmitted AIS signals has a constant envelope form as

$$s(t) = e^{j\theta(t)}, \tag{1}$$

where $\theta(t)$ is the phase given by

$$\theta(t) = \pi h \int_{-\infty}^{t} \sum_{n=-\infty}^{+\infty} a_n g(\tau - nT) d\tau, \tag{2}$$

where h is the modulation index equal to 0.5, and $g(t)$, a pulse of unit area, is the response of a Gaussian filter to a unit amplitude rectangular pulse of duration T, where T is the symbol period. The GMSK
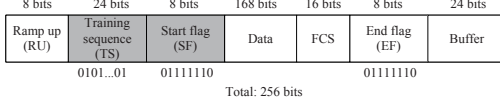
Fig. 1. The default AIS message.

modulation is described by the bandwidth-time product BT, where B is the bandwidth of the Gaussian filter. AIS uses two possible BT values 0.3 or 0.4.

Scenario: In AIS receivers, the received data are processed frame by frame. Here, an antenna array with M elements is assumed on the satellite. While collecting continuous data frames along the time line (see Fig. 2), we consider the target data frame (e.g. Data frame 1 in Fig. 2) containing d asynchronous AIS messages each from one of the d users. The received signals are demodulated to baseband and sampled at period $T_s = T/P$, where P is the over-sampling ratio. Collecting PN samples over N symbol periods, we form the data model for the target data frame,

$$\mathbf{X} = \mathbf{HG}(\mathbf{S} \odot \mathbf{\Phi}) + \mathbf{N}, \tag{3}$$

where $\odot$ is the Schur-Hadamard (pointwise multiplication) operator, $\mathbf{X} = [\mathbf{x}_1, \mathbf{x}_2, \ldots, \mathbf{x}_{PN}] \in \mathbb{C}^{M \times PN}$, $\mathbf{x}_n = \mathbf{x}(nT_s), 1 \le n \le PN$, is the received data matrix, $\mathbf{H} = [\mathbf{h}_1, \mathbf{h}_2, \ldots, \mathbf{h}_d] \in \mathbb{C}^{M \times d}$ is the array response matrix, $\mathbf{G} = \mathrm{diag}\{g_1, g_2, \cdots, g_d\} \in \mathbb{R}^{d \times d}$ contains the source power, $\mathbf{S} = [\mathbf{s}_1^H, \mathbf{s}_2^H, \ldots, \mathbf{s}_d^H]^H \in \mathbb{C}^{d \times PN}$ is the source data matrix,

$$\mathbf{\Phi} = \begin{bmatrix} 1 & \varphi_1^1 & \cdots & \varphi_1^{PN-1} \\ 1 & \varphi_2^1 & \cdots & \varphi_2^{PN-1} \\ \vdots & \vdots & \ddots & \vdots \\ 1 & \varphi_d^1 & \cdots & \varphi_d^{PN-1} \end{bmatrix}, \varphi_k = \mathrm{e}^{j2\pi\Delta f_k T_s}, \tag{4}$$

contains the Doppler phase shifts for sources, and $\mathbf{N} \in \mathbb{C}^{M \times PN}$ is the white Gaussian noise matrix. Although all AIS messages are synchronized by the universal time control (UTC) (e.g. GPS), the received messages still have large difference in time of arrivals (TOA), so $\mathbf{S}$ contains absent samples from sources (See Fig. 2).

For a LEO satellite orbiting at altitude 600km, the overlapping between messages from adjacent time slots can be up to 74 bits (29% overlapping), the Doppler frequency shift Δf_k can be up to ± 3.7kHz, and the variance in signal-to-noise ratio (SNR) can be up to around 10dB and even larger if one takes into account the spinning of the satellite, wave polarization and ionospheric scintillation [14]. Despite of the large variance in SNR, AIS signals usually have a high SNR from 15dB to 25dB.

3 BASEBAND MULTI-USER RECEIVER

In this section, we propose a baseband multi-user receiver for space detection of AIS messages. The scheme is illustrated in Fig. 3.

3.1 RANK TRACKING

In order to determine the start of data frames, we use the subspace tracking algorithm proposed in [9] to track the rank change of the data matrix $\mathbf{X}_{rt} \in \mathbb{C}^{M \times PN_w}$ of a sliding window with fixed length PN_w samples long, $M \ll PN_w \ll PN_p$. Given the threshold $\gamma_1 = \beta_1\sigma_n(\sqrt{PN_w} + \sqrt{M})$ on the noise power σ_n^2 [9], we continuously append new coming vectors $\mathbf{x}_n$ from antennas to and remove old vectors from $\mathbf{X}_{rt}$ in the following compact SURV [9]

$$[\overset{+}{\gamma_1\mathbf{I}} \ \overset{-}{\mathbf{X}_{rt}}] \mathbf{\Theta}_1 = [\mathbf{Q}_{\mathbf{A}_1} \ \mathbf{Q}_{\mathbf{B}_1}][\overset{M-\hat{d}}{\mathbf{L}_{\mathbf{A}_1}} \ \overset{\hat{d}}{\mathbf{L}_{\mathbf{B}_1}}], \tag{5}$$
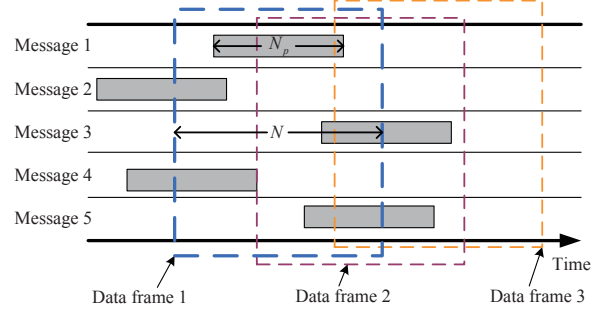
Fig. 2. The collected continuous data frames.
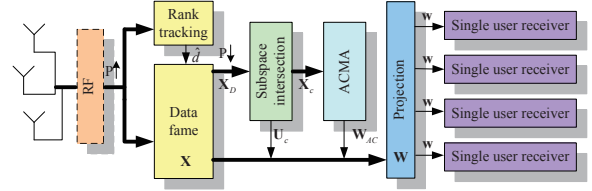
Fig. 3. Block diagram of the baseband multi-user receiver.

where the sign + and - above matrices denote the positive and negative signatures of the columns in those matrices, $\mathbf{\Theta}_1$ is part of a **J**-unitary matrix [10, 15], $[\mathbf{L}_{\mathbf{A}_1} \ \mathbf{L}_{\mathbf{B}_1}] \in \mathbb{C}^{M \times M}$ is a lower triangular matrix, and $[\mathbf{Q}_{\mathbf{A}_1} \ \mathbf{Q}_{\mathbf{B}_1}] \in \mathbb{C}^{M \times M}$ is a unitary matrix. $\hat{d}$ is the rank of the matrix $\mathbf{X}_{rt}$ and the estimated number of users in the sliding window.

Whenever a rank rising edge is detected or the rank is saturated $\hat{d} = M$, one data frame $\mathbf{X}$ with length $PN = 2PN_p$ samples long is collected from the received data buffer. The start of the data frame is set to $0.5PN_p$ samples ahead of the rank rising edge. The minimum time shift between two continuous data frames is set to $0.5PN_p$ samples. This tracking algorithm can resist for a long time (up to hours) in a DSP processor before the next resetting. It runs at a clock speed PN_w times slower than the singular value decomposition (SVD).

The computational complexity of this block is of $O(M^2)$ per vector update.

3.2 SUBSPACE INTERSECTION

The collected data frame contains incomplete asynchronous AIS messages which destroy the convergence of ACMA [10]. The subspace intersection block is applied to remove these incomplete data in $\mathbf{X}$. The steps are as follows

Step 1. Downsample $\mathbf{X}$ by P to form matrix $\mathbf{X}_D \in \mathbb{C}^{M \times N}$, and project $\mathbf{X}_D$ onto its principal subspace $\underline{\mathbf{X}} = \mathbf{U}_p^H\mathbf{X}_D \in \mathbb{C}^{\hat{d}_p \times N}$.

Step 2. Divide $\underline{\mathbf{X}}$ from its center into two submatrices, $\underline{\mathbf{X}} = [\underline{\mathbf{X}}_1 \ \underline{\mathbf{X}}_2]$.

Step 3. Form two compact SURVs

$$[\overset{+}{\alpha\underline{\mathbf{X}}_1} \ \overset{-}{\underline{\mathbf{X}}_2} \ \overset{-}{\gamma_3\mathbf{I}}] \mathbf{\Theta}_2 = [\mathbf{Q}_{\mathbf{A}_2} \ \mathbf{Q}_{\mathbf{B}_2}][\overset{+}{\mathbf{L}_{\mathbf{A}_2}} \ \overset{-}{\mathbf{L}_{\mathbf{B}_2}}], \tag{6}$$

$$[\overset{+}{\alpha\underline{\mathbf{X}}_2} \ \overset{-}{\underline{\mathbf{X}}_1} \ \overset{-}{\gamma_3\mathbf{I}}] \mathbf{\Theta}_3 = [\mathbf{Q}_{\mathbf{A}_3} \ \mathbf{Q}_{\mathbf{B}_3}][\overset{+}{\mathbf{L}_{\mathbf{A}_3}} \ \overset{-}{\mathbf{L}_{\mathbf{B}_3}}], \tag{7}$$

where $\alpha \ge \frac{\sqrt{0.5N} + \sqrt{M}}{\sqrt{0.5N} - \sqrt{M}}$, $\gamma_3 = \sqrt{\alpha^2 - 1}\gamma_2$, $\gamma_2 = \beta_2\sigma_n$.

$(\sqrt{0.5N} + \sqrt{M})$ [10].

Step 4. *Subspace intersection* [16]: Compute SVD $[\mathbf{Q_{A_2}} \quad \mathbf{Q_{A_3}}] = \mathbf{U}\text{diag}(\sigma_i)\mathbf{V}^H$. Let $\mathbf{U}'_c = \mathbf{U}(:,1:\hat{d}_c)$ such that $\sigma_i \geq \sqrt{2}$, $1 \leq i \leq \hat{d}_c$, and $\sigma_i < \sqrt{2}$, $\hat{d}_c + 1 \leq i \leq \hat{d}_p$. The columns of $\mathbf{U}'_c$ is the orthonormal basis of the interference-free subspace for the complete AIS messages. $\hat{d}_c$ is the estimated number of useful users.

Step 5. Do projection $\mathbf{X}_c = \mathbf{U}_c^H \mathbf{X}_D$, $\mathbf{U}_c = \mathbf{U}_p \mathbf{U}'_c$.
The computational complexity of this block is of $O(M^2 N)$.

3.3 BLIND SOURCE SEPARATION

Since $\mathbf{X}_c$ only contains complete messages, the data matrix becomes stationary for the followed ACMA. We use N_{AC} ($N_{AC} > M^2$) columns in the center of $\mathbf{X}_c$ for ACMA [11]. ACMA uses the property of AIS signals $|s(t)| = 1$ to compute second order tensors of the received data and forms a tall matrix $\mathbf{P}$. The beamformers $\mathbf{W}_{AC} \in \mathbb{C}^{\hat{d}_c \times \hat{d}_c}$ are found by solving a joint diagonalization problem that finds the vectors best spanning $\ker(\mathbf{P})$. Then we have the beamformer matrix $\mathbf{W} = \mathbf{U}_c \mathbf{W}_{AC} = [\mathbf{w}_1, \mathbf{w}_2, \ldots, \mathbf{w}_{\hat{d}_c}] \in \mathbb{C}^{M \times \hat{d}_c}$.

The computational complexity of this block is of $O(\hat{d}_c^4 N_{AC})$.

3.4 SINGLE USER RECEIVER

Now, the collision-free k-th user data $\hat{\mathbf{s}}_k = \mathbf{w}_k^H \mathbf{X}$ is ready for detection. First, $\hat{\mathbf{s}}_k$ is truncated to a shorter sequence (we still use $\hat{\mathbf{s}}_k$ to denote this sequence) with a length slightly larger than PN_p by doing a coarse search on it to find the ramp up part of the AIS message (which is a simple energy detection method). Subsequently, we apply the algorithm proposed in [8] (see Fig. 4), which is simple and robust to Doppler phase shift, on $\hat{\mathbf{s}}_k$. This algorithm consists of two steps.

Step 1. The first step is frame synchronization. It uses the 1-bit differential version of the modulated synchronization sequence $\mathbf{v}$ (TS and SF) to correlate the 1-bit differential version of $\hat{\mathbf{s}}_k$ [13]. Define the k-th bit differential transform

$$\Delta_k y(t) = y(t)y^*(t - kT). \quad (8)$$

We have

$$R(n) = \Delta_1 \hat{s}_k(n) * \Delta_1 v^*(-n)/\text{length}(\mathbf{v}), \quad (9)$$

where $*$ denotes the convolution operator and $(\cdot)^*$ denotes the conjugate operator. The peak position found in $|R(n)|$ is the estimated time delay $\hat{\tau}_k = \hat{n}_k T_s$ and $R(\hat{n}_k) = |A| e^{-j2\pi\Delta\hat{f}_k T}$ provides the estimate of Doppler phase shift. [8] also deals with the case with initial differential coding status $a_0 = -1$, which is solved by the conjugate correlation in (9).

Step 2. Then in the second step, a 2-bit differential detector (DD) [13] is applied on $\hat{\mathbf{s}}_k$.

$$\hat{b}_{kn} = -\text{sign}(\Delta_2 \hat{s}_k(n + \hat{n}_k)e^{-j4\pi\Delta\hat{f}_k T} - o), \quad (10)$$

where $o = 0.2$ [8, 13]. The demodulated data are mapped to binary data and then decoded by the AIS message decoder. Only the messages that pass the CRC check are recorded. The computational complexity of this block is of $O(PN)$.

4 SIMULATION RESULTS

In this section, we test our proposed receiver in the exact AIS model we developed based on [12]. The simulation results of three receivers are compared, which are our complete proposed receiver (MU+SI), our proposed receiver but without subspace intersection (MU) and
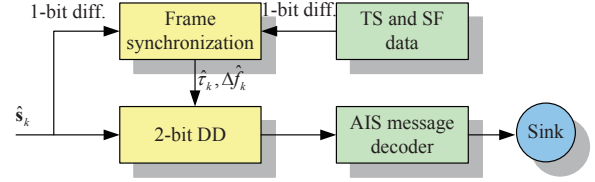
Fig. 4. Block diagram of the single user receiver.

Table 1. The simulation configuration.

Carrier frequency	162.025MHz
Channel bandwidth	25kHz
Modulation	9.6kbps GMSK
BT	0.3
Satellite altitude	600km
Satellite speed	7561.65m/s
Orbit period	5792.52s
Number of ships in FoV	2,000 and 10,000
Number of cells covering FoV	5476
Radius of FoV	1437.74 nautical miles
Maximum ship visible time	704s
Ship transmission interval	60s
Message length	256bits
Ship transmitter power	12.5W
Ship antenna type	Half-wave dipole
Number of satellite antennas M	1 to 10
Satellite antenna spacing	Half wavelengths
Maximum SNR at the receiver	25dB

the single user receiver (SU) [8]. The single user receiver is implicitly compared in the simulation results, which corresponds to MU with one antenna. The simulation model is configured as listed in Table 1. For the MU receivers, the antenna array consists of two linear subarrays crossing each other locating in the plane parallel to FoV. Each subarray has $M/2$ dipoles spacing at half wavelengths. One of the subarrays is parallel to the satellite velocity vector v_{sat}. We set $P = 8$, $N_w = 20$, $N_{AC} = 200$, $\alpha = 8$, $\beta_1 = 1.2$, and $\beta_2 = 1.3$. The performance measure is the ratio of the number of successfully decoded messages to the number of sent messages.

Fig. 5 shows the simulation scenario. The outer big blue circle denotes the margin of FoV and the small blue circles denote the detected ship positions in FoV. The satellite velocity vector v_{sat} is parallel to the vertical axis. The test environment is a dynamic model where ship positions are randomly generated in the initialization and the ships are moving backwards opposite to the satellite velocity vector. The number of ships in FoV is fixed. New ships with randomly generated positions at the top margin of FoV continuously come into FoV while ships of the same number are moving out at the bottom of FoV. Every ship has a unique ship ID. In Fig. 5, the number of ships in FoV is 2,000, the simulated system time period is 100 seconds, and the receiver type is MU+SI with 10 antennas.

Fig. 6 shows the performance of receivers with 2,000 ships in FoV as a function of the number of antennas. According to [3], the detection possibility of SU drops dramatically at 2,000 ships in FoV with 6 seconds interval and in [17], a 1 to 3 hours interval is recommended to improve the performance. Fig. 6 shows a 60 seconds interval is long enough for MU+SI to provide satisfactory performance. It is seen that the number of ships detected by the MU receivers grows significantly by the number of antennas. MU+SI outperforms MU as expected and shows detection possibility close to 1 at $M = 10$ (the number of detected ship IDs is also shown).

Fig. 7 shows the performance of receivers with 10,000 ships in FoV as a function of the number of antennas. The number 10,000 is
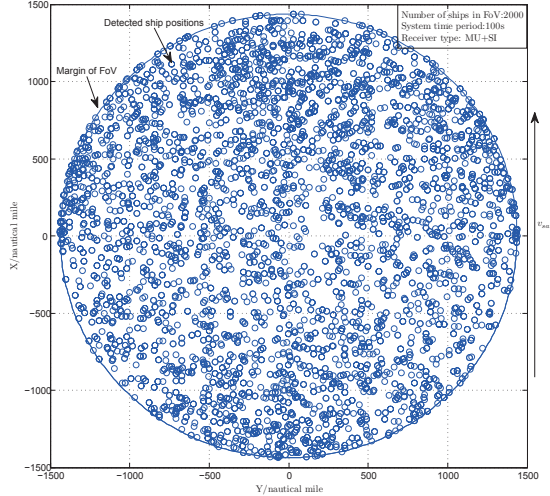
Fig. 5. The simulation scenario.
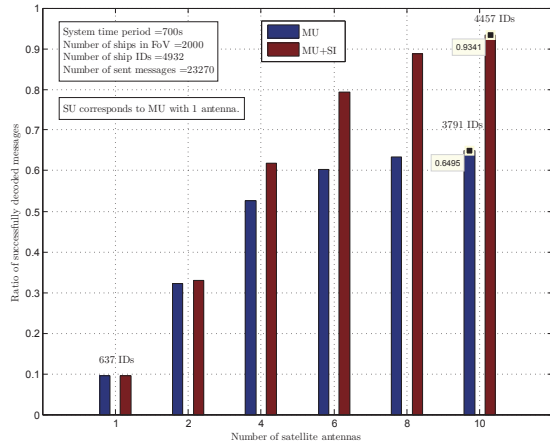
Fig. 6. The performance of receivers with 2,000 ships in FoV.

close to the number of ships in FoV at North Sea, which is a worst case. It is seen that SU detects very few ships and MU+SI outperforms MU. Especially, the improvement by MU+SI compared with MU is 125% at $M = 10$.

5. CONCLUSION

We proposed a multi-user receiver for space detection of AIS messages on LEO satellites. The receiver explored the spatial multiplexing in the considered asynchronous nonstationary scenario. It used rank tracking and subspace intersection based on the signed URV decomposition ahead of blind source separation to provide robust separation of user data. The receiver was tested in an exact dynamic AIS model. The simulation results showed that this receiver was robust to the collision of messages, and significantly improved the detection performance compared with the previous single user receiver.

6. REFERENCES

[1] *RECOMMENDATION ITU-R M.1371-2: Technical characteristics for a universal shipborne automatic identification system using time division multiple access in the VHF maritime mobile band*, ITU Std., 2006.
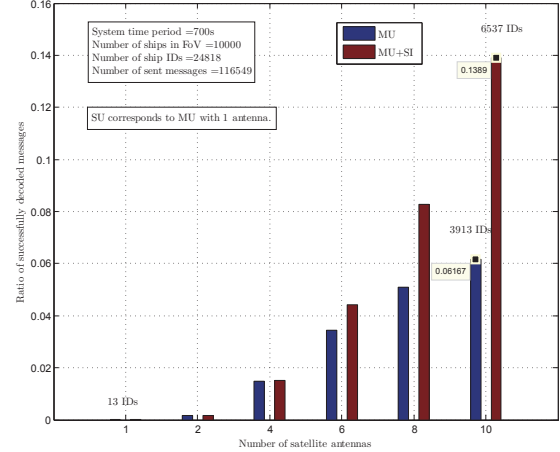
Fig. 7. The performance of receivers with 10,000 ships in FoV.

[2] O. F. H. Dahl, "Space-based AIS receiver for maritime traffic monitoring using interference cancellation," Master's thesis, Norwegian University of Science and Technology, Department of Electronics and Telecommunications, 2006.

[3] *REPORT ITU-R M.2084: Satellite detection of automatic identification system messages*, ITU Std., 2006.

[4] M. A. Cervera, A. Ginesi, and K. Eckstein, "Satellite-based vessel automatic identification system: A feasibility and performance analysis," *Int. J. Satell. Commun. Network.*, 2009.

[5] T. Eriksen, G. Høye, B. Narheim, and B. J. Meland, "Maritime traffic monitoring using a space-based AIS receiver," *Acta Astronautica*, vol. 58, no. 10, pp. 537–549, 2006.

[6] M. Gallardo and U. Sorger, "Coherent receiver for AIS satellite detection," in *4th Int. Symp. on Commun., Control and Signal Process.*, Mar. 2010, pp. 1–4.

[7] D. J. Nelson and J. R. Hopkins, "GMSK co-channel demodulation," in *Proc. SPIE 7444*, 2009, p. 74440V.

[8] J. E. Hicks, J. S. Clark, J. Stocker, G. S. Mitchell, and P. Wyckoff, "AIS/GMSK receiver on FPGA platform for satellite application," in *Proc. SPIE 5819*, 2005, p. 403.

[9] M. Zhou and A.-J. van der Veen, "Stable subspace tracking algorithm based on signed URV decomposition," in *Proc. IEEE Int. Conf. Acoust., Speech, Signal Process.*, Prague, Czech Republic, May 2011, pp. 2720–2723.

[10] ——, "Improved subspace intersection based on signed URV decomposition," in *Proc. of the Asilomar Conf. on Signals, Syst., and Comput.*, Pacific Grove, California, USA, Nov. 2011.

[11] A.-J. van der Veen and A. Paulraj, "An analytical constant modulus algorithm," *IEEE Trans. Signal Process.*, vol. 44, no. 5, pp. 1136–1155, May 1996.

[12] M. Zhou and R. van Leuken, "SystemC-AMS model of a dynamic large-scale satellite-based AIS-like network," in *Forum on specification and Design Languages*, Oldenburg, Germany, Sept. 2011, pp. 24–31.

[13] M. Simon and C. Wang, "Differential detection of Gaussian MSK in a mobile radio environment," *IEEE Trans. Veh. Technol.*, vol. 33, no. 4, pp. 307–320, Nov. 1984.

[14] J. Aarons, "Global morphology of ionospheric scintillations," *Proc. IEEE*, vol. 70, no. 4, pp. 360–378, Apr. 1982.

[15] A.-J. van der Veen, "A Schur method for low-rank matrix approximation," *SIAM J. Matrix Anal. Appl.*, vol. 17, no. 1, pp. 139–160, 1996.

[16] G. H. Golub and C. F. Van Loan, *Matrix computations (3rd ed.)*. Baltimore, MD, USA: Johns Hopkins University Press, 1996.

[17] *RECOMMENDATION ITU-R M.2169: Improved Satellite Detection of AIS*, ITU Std., 2009.